Available online at www.sciencedirect.com
ScienceDirect
International Journal of Mass Spectrometry 263 (2007) 94–100
International Journal of Mass Spectrometry
www.elsevier.com/locate/ijms

Simultaneous monitoring of the radial modes of the ion motion and their manipulation in Penning traps by FT-ICR mass spectrometry

Martin Breitenfeldt [a,*], Falk Ziegler [a], Alexander Herlert [b], Gerrit Marx [a], Lutz Schweikhard [a]

[a] *Institut für Physik, Ernst-Moritz-Arndt-Universität, 17487 Greifswald, Germany*
[b] *Physics Department, CERN, 1211 Geneva 23, Switzerland*

Received 15 November 2006; received in revised form 4 January 2007; accepted 5 January 2007
Available online 12 January 2007

Abstract

It is demonstrated how FT-ICR MS can be used to monitor both the coherent magnetron motion and the cyclotron motion of ions stored in a Penning trap. By use of the ICR signal intensity at the magnetron frequency, ν_-, and the reduced cyclotron frequency, ν_+, the manipulation of the ion motion by dipolar, quadrupolar, and octupolar excitation has been followed. In particular, the conversion between the magnetron and the cyclotron motion by quadrupolar and octupolar excitation at the corresponding resonance frequencies $\nu_c = \nu_+ + \nu_-$ and $2\nu_c$, respectively, has been observed by detection of the magnetron and the cyclotron signal. While the ion motion under the influence of a quadrupolar excitation has already been studied extensively, the octupolar excitation has been introduced only recently. As compared to other techniques, such as the time-of-flight ion-cyclotron-resonance detection method, FT-ICR MS allows to simultaneously investigate the influence of an excitation on the cyclotron und the magnetron motional modes.
© 2007 Elsevier B.V. All rights reserved.

Keywords: Penning trap; Ion motion; FT-ICR; Dipolar/quadrupolar/octupolar excitation

1. Introduction

Fourier transform ion cyclotron resonance mass spectrometry (FT-ICR MS) has proven to be a highly effective and efficient method in many branches of analytical chemistry [1–4]. As related technique, the narrow-band detection of induced image currents is used for precision mass spectrometry directed towards the investigation of fundamental questions in physics [5–9]. These experiments all build on the storage of ions in Penning traps [10]. FT-ICR can be used to further investigate the principles of this device [11–15], and this tradition is continued in the present study.

In general, the standard FT-ICR MS measurements are only concerned with the signal at the reduced cyclotron frequency ν_+. Harmonics [16–19] and combinations [20] of ν_+ and the magnetron frequency ν_- have been considered, but for analytical applications they are of rather limited usefulness [21] or even a nuisance and unwanted source of confusion [22]. Thus, experiments directed towards the detection of these signals by application of appropriate detection geometries have not been followed up extensively. The present investigation is no exception, i.e., the detection is performed in standard (dipolar) FT-ICR detection geometry.

However, harmonics and frequency combinations may not only be considered for the detection, but also for the excitation of the ion motion [23]. In particular, the application of the quadrupolar rf excitation at $\nu_{rf} = \nu_+ + \nu_-$ is a very important technique in both analytical chemistry [24–26] and fundamental nuclear-physics studies, where it has been invented [27]. Higher multipoles, like octupolar fields, are presently studied [28,29].

The dipolar FT-ICR detection geometry allows to look not only at the signal at the reduced cyclotron frequency but, in addition, also at the magnetron signal. As this latter signal is in first order not mass-specific, it is usually not considered. However, with the approach to use a combination of frequencies for a conversion between the motional modes as applied in fundamental-physics experiments, both the cyclotron and the magnetron signal are of interest. In the present study they are both monitored simultaneously and it is demonstrated how the dipolar, quadrupolar, and octupolar excitation can be investigated with

* Corresponding author.
E-mail address: martin.breitenfeldt@cern.ch (M. Breitenfeldt).

1387-3806/$ – see front matter © 2007 Elsevier B.V. All rights reserved.
doi:10.1016/j.ijms.2007.01.003

respect to the influence of such standard and novel excitation schemes on the two motional modes and their coupling.

2. Experimental setup and procedure

The experiments have been performed at ClusterTrap [30,31] which has been constructed and further developed for the investigation of metal clusters [32–34]. For the present measurements the highly sensitive time-of-flight analysis, that is usually performed at this setup for single-ion detection, has been replaced by a broad-band FT-ICR detection. In order to have a sufficiently large number of ions in each experimental cycle to obtain a measurable ion signal, Ar^+ ions have been produced by electron-impact ionization of argon gas in the trap volume.

Fig. 1 shows an overview of the setup with the main parts used in this investigation. Fig. 2 (top) illustrates the segmentation of the ring electrode and the connections for the dipolar rf excitation of the ion motion and the image-signal pickup. The asymptotically symmetric Penning trap [40] uses hyperbolically shaped electrodes with an inner ring diameter of 40 mm. With a magnetic field strength of 5 T and a trapping potential of 30 V applied between the ring and the end-cap electrodes, the reduced cyclotron frequency and the magnetron frequency of Ar^+ are $\nu_+ = 1907.25$ kHz and $\nu_- = 2.44$ kHz, respectively.

As mentioned above, the present work aimed at the investigation of the radial motions of stored ions after the interaction with radio-frequency fields. Especially the conversion from one mode into the other by use of a quadrupolar or octupolar excitation was studied. In general, the experimental event sequence consisted of the following steps:

(1) ionization of argon atoms by application of an axial electron beam;
(2) radio-frequency (rf) excitation for 10 ms in dipolar geometry at the magnetron frequency, if a quadrupolar or octupolar rf excitation is subsequently applied;
(3) excitation for 10 ms with either (a) dipolar, (b) quadrupolar or (c) octupolar geometry;
(4) broad-band FT-ICR detection.

All excitation events were performed with single-frequency signals. For a measurement series either the excitation amplitude was varied or the frequency was scanned in small steps around the expected resonance frequency.

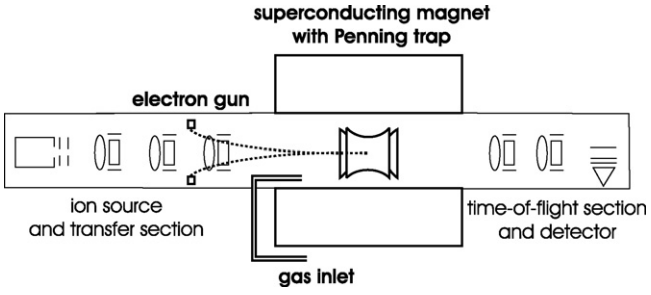

Fig. 1. Overview of ClusterTrap with the parts used in this work indicated in bold face.

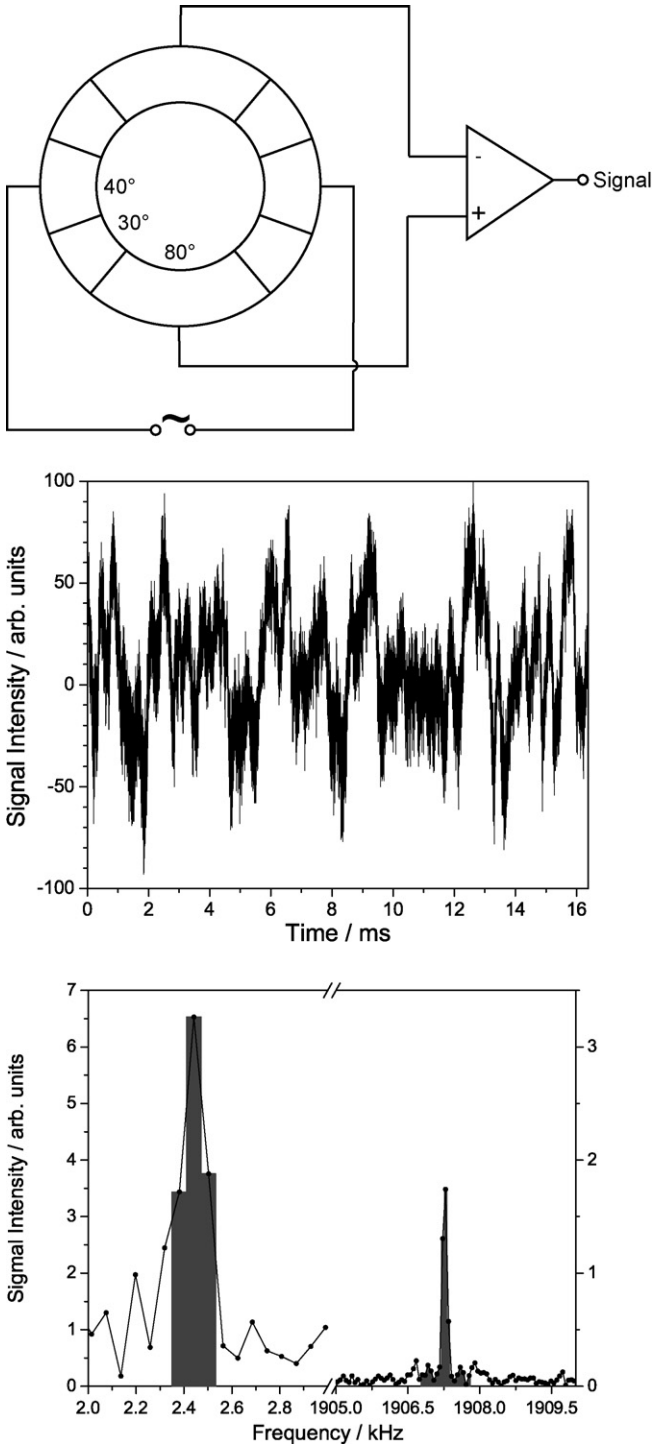

Fig. 2. (Top) Overview of the segmentation of the ring electrodes with the connections for the dipolar excitation (40° segments) and the FT-ICR detection (80° segments). (Center) Ion signal in the time domain (transient). (Bottom) Low-frequency and high-frequency range of the frequency spectrum (in the vicinity of the magnetron and the reduced cyclotron frequency, respectively) as deduced from the transient shown in the center graph. The data points integrated for further evaluation of the signal intensity are indicated by the shaded areas.

For the ionization in step (1) argon was continuously leaked into the trap volume, which resulted in a pressure of about $p = 4 \times 10^{-8}$ h Pa. This was the limiting factor of the achievable resolving power for both excitation resonances ("front-end"

resolving power [35,36]) as well as for the FT-ICR transient signal duration. The dipolar excitation signals are applied for the creation of a coherent ion motion at the magnetron frequency as given in step (2) of the event sequence. The 10-ms excitation signal was created by a SRS DS345 frequency generator and a home-built phase splitter and applied with opposite polarity on the opposing 40° ring segments (see Fig. 2 (top)).

The excitation signals of step (3) were produced by a second frequency generator (Rhode & Schwarz AM300). For the dipolar excitation in step (3a) the rf signal was applied as in step (2). The quadrupolar (3b) and octupolar excitations (3c) with a duration lengths of 10 ms were applied on the 30° segments, where one pair of opposing segments was used for the quadrupolar excitation and all four 30° segments for the octupolar excitation. In the latter case, the excitation amplitude was increased by a rf amplifier (ENI, model 2100) to reach the amplitude necessary for a full conversion of the motional modes. Note that the geometrical configurations are a compromise with respect to the present segmentation of the ClusterTrap electrodes and easy switching between the different modes. For none of these modes the applied geometrical configurations are ideal. However, a Fourier analysis shows that the multipole fields in question are created by these configurations with a sufficiently large fraction. As discussed earlier [37,38] it is sufficient to use only one polarity for a quadrupolar excitation. For the octupolar mode the same arguments apply. In both cases, single-polarity excitation leads to an additional parametric effect [39]. However, as the present studies have not been performed in the vicinity of resonance frequencies of the parametric excitation modes, no complications due to such modes are expected.

After the excitation in step (3) the ions moved coherently along their specific trajectories. In the last step of the sequence the resulting image-charge signal was picked up on the two opposing 80° segments for differential amplification as shown in Fig. 2 (top). The signal was fed into a home-built broad-band difference amplifier and stored by a transient recorder (FastComtech, PCI.212). The transients were analyzed by use of a Lab View based fast Fourier transform (FFT) software.

Each transient consists of 65,536 data points from a 12-bit ADC at a sampling rate of 4 MHz, corresponding to a transient length of 16.4 ms (see Fig. 2 (center)). From this transient in the time domain the Fourier transform is calculated by use of an FFT algorithm provided by LabVIEW. Both the cyclotron and the magnetron signal are visible in the frequency spectrum and the peak area, as indicated in Fig. 2 (bottom), is used as a measure of the signal strength. In case of the magnetron motion the signal intensity is calculated from the values of the data point at the eigenfrequency and of those at the two neighboring points. For the cyclotron motion, where the signal is in a less noisy frequency region, it is possible to include the first Fourier sidebands and to determine the signal strength from the data point at the eigenfrequency and eight neighboring points to each side in the frequency spectrum, which corresponds to a frequency range of ±500 Hz (see Fig. 2 (bottom)). The signal intensities quoted in the following sections are each an average of five independent measurements.

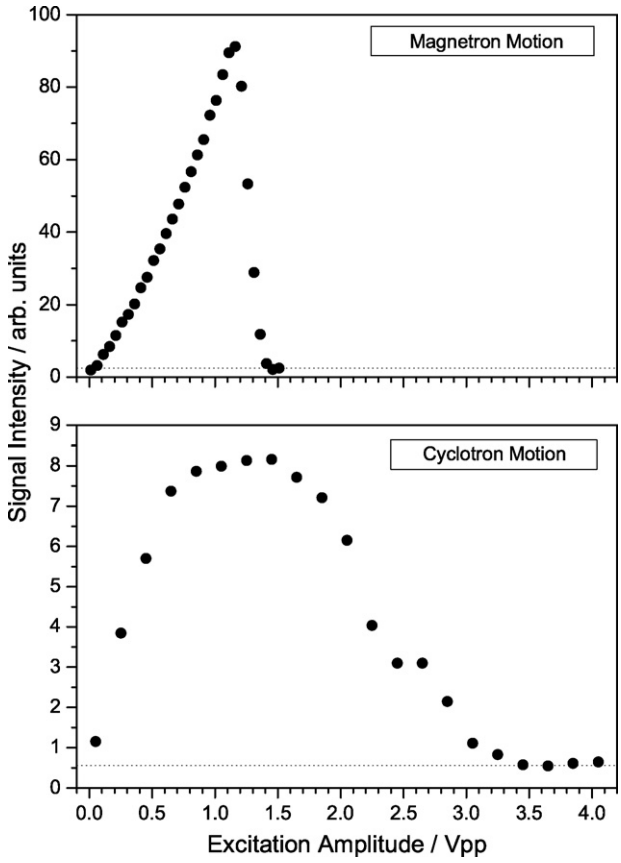

Fig. 3. Intensity of the magnetron (top) and the cyclotron signal (bottom) as a function of the amplitude (as given by the frequency generator) of the resonant dipolar excitation at $\nu_{rf} = 2.44$ kHz and $\nu_{rf} = 1907.25$ kHz, respectively. The dashed lines give the noise level of the signal intensities as determined from measurements without an excitation of the ion motion.

3. Results and discussion

3.1. Dipolar excitation

Fig. 3 (top) shows the intensity of the magnetron signal as a function of excitation amplitude for the dipolar excitation at $\nu_{rf} = 2.44$ kHz. As the signal in the standard FT-ICR dipolar detection mode is proportional to the radius of the ion orbit and as this radius is proportional to the excitation amplitude, it is expected and observed that the signal strength (in the standard magnitude spectrum [41]) is proportional to the excitation amplitude. When the magnetron radius approaches the trap radius, the ions collide with the ring electrode and are lost from the trap. Thus, at the corresponding excitation amplitude the ion signal breaks down. Note that there is a slight non-linear increase of the magnetron signal which may result from the friction force due to the ions colliding with the residual gas atoms [23].

The bottom of Fig. 3 shows the cyclotron-signal intensity after a resonant dipolar excitation. For a moderate excitation amplitude the data points are on a straight line, similar as for the magnetron excitation. However, when the excitation amplitude is increased the signal intensity levels off. Obviously, the damping force increases as a function of the cyclotron radius, which is expected as this is proportional to the ion velocity. Thus,

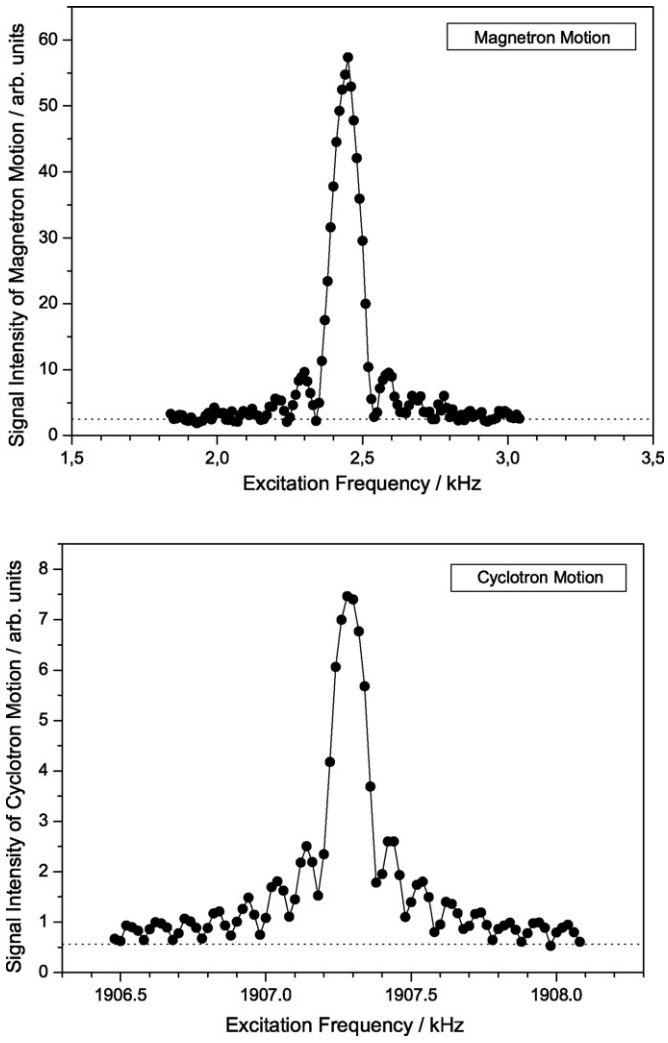

Fig. 4. Signal intensity of the magnetron (top) and cyclotron motion (bottom) as a function of the excitation frequency for the dipolar-excitation mode. The data points are connected by straight lines to guide the eye. The dashed lines illustrate the level of the signal intensities as determined from measurements without an excitation of the ion motion.

the collisions result in a range of excitation amplitude where the strength of the FT-ICR signal at the reduced cyclotron frequency is more or less constant. Only when the excitation amplitude is increased even further, the ion orbits increase so fast that the ions reach the electrodes in times short compared to the collision times, i.e., the length of the trajectories decreases below the mean free path. For these amplitudes the ions are lost during the excitation and the FT-ICR signal disappears.

In the following the excitation amplitude was kept fixed and the frequency of the rf excitation was varied. Fig. 4 (top) shows the magnetron signal intensity as a function of the excitation frequency. The amplitude (0.8 V_{pp}) was chosen such that the radius of the magnetron motion remains moderate and other effects, e.g., the friction as mentioned above or an eigenfrequency shift due to image charges [42] are negligible.

The observed line shape of the magnetron resonance is the well-known "sinc" function [41]. The number of sidebands observed is limited by the noise level around the magnetron frequency as mentioned above. In Fig. 4 (bottom) a corresponding frequency scan is shown for the resonance at the reduced cyclotron frequency. As expected, the shape of the resonance curve is the same as in the case of the magnetron excitation. The central peaks of both resonance curves have the expected FWHM of about 100 Hz for an excitation duration of 10 ms.

3.2. Quadrupolar excitation

As described above, the FT-ICR technique allows the simultaneous detection of the magnetron and the cyclotron signal with a single transient. Thus, in the case of the quadrupolar excitation it is possible to monitor the conversion from one mode into the other by observing the two signal intensities as a function of, e.g., the excitation amplitude, where the frequency is fixed to the expected resonance frequency $\nu_+ + \nu_- = \nu_c = 1909.7$ kHz. For these measurements the ions are prepared to perform an initial magnetron motion by a dipolar rf excitation at $\nu_{rf} = \nu_- = 2.44$ kHz, which corresponds to step (2) of the event sequence as described in Section 2.

The result of the subsequent quadrupolar excitation is shown in Fig. 5. The ions start with a pure magnetron motion. As expected, the signal intensities of the magnetron and the cyclotron motion show periodic changes as a function of the excitation amplitude, where magnetron-intensity minima correspond to cyclotron-intensity maxima and vice versa indicating the conversion between the two motional modes [27].

For three different excitation amplitudes, marked in the figure with (1), (2) and (3), the low- and high-frequency ranges of the FFT spectra are given for further illustration. Frequency spectrum (1) shows the situation after one conversion. Thus, the low-frequency range of the spectrum, where a magnetron signal would appear, shows no signal. In contrast, in the high-frequency range a clear signal at the reduced cyclotron frequency is observed. Frequency spectrum (2) shows the case for a higher excitation amplitude for which the ion motion has been almost converted back to a pure magnetron motion. In the low-frequency range a signal appears at the expected magnetron frequency value. At high frequencies the signal intensity at the reduced cyclotron frequency has decreased to almost zero. A further increase of the excitation amplitude results in a second conversion to the cyclotron motion as shown in frequency spectrum (3), where both the magnetron and the cyclotron signal are visible.

Fig. 6 shows the result of a scan of the excitation frequency for the conversion by use of a quadrupolar rf excitation. The signal intensity of the cyclotron motion shows the expected sinc shape. The magnitude of the central peak is somewhat low as compared to the intensity of the sidebands probably due to damping during excitation and detection.

The resonance shape of the magnetron signal is not as pronounced as that of the cyclotron signal. The noise level at the magnetron frequency is rather high with respect to the signal intensity. Thus, the sidebands disappear in the statistical fluctuations.

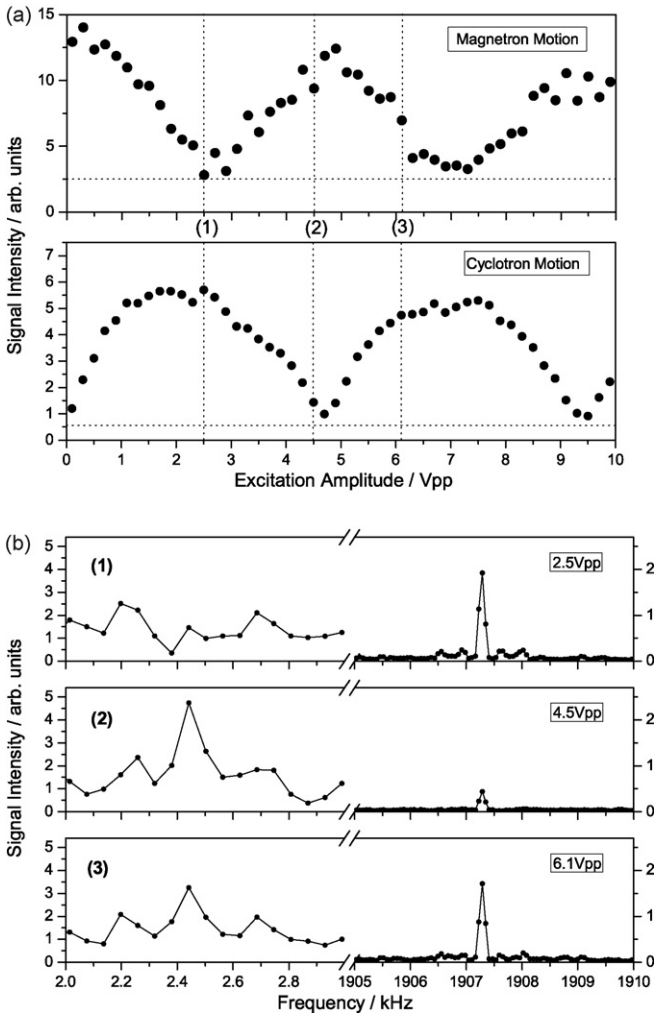

Fig. 5. (a) Signal intensity of the magnetron (top) and cyclotron motion (bottom) as a function of the rf quadrupolar excitation amplitude at the excitation frequency $\nu_{rf} = \nu_c = 1909.7$ kHz. The dashed lines indicate the noise level for the eigenmotion signals. (b) Low- (left side) and high-frequency range (right side) of the spectra at the amplitudes of 2.5, 4.5 and 6.1 V_{pp}. In each case the frequency ranges for the magnetron and the reduced cyclotron frequency are shown.

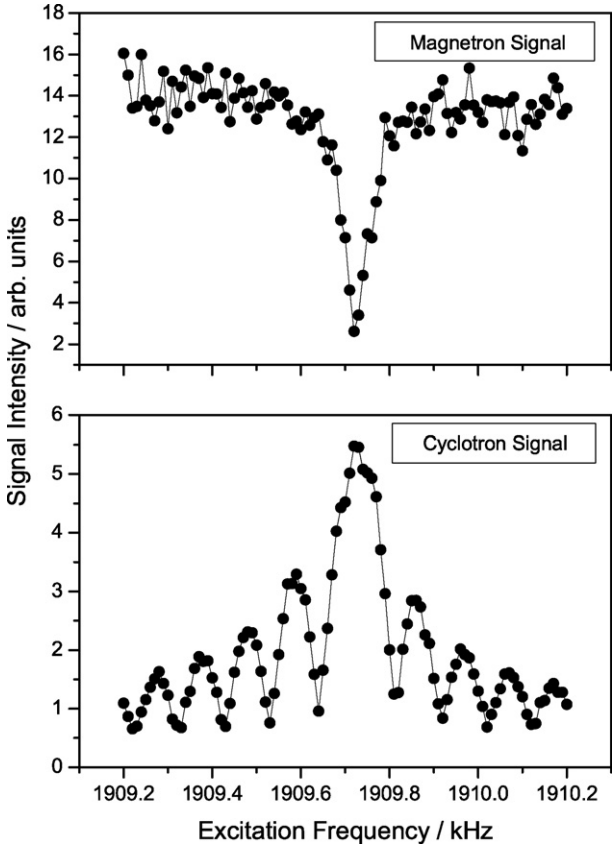

Fig. 6. Signal intensity at the magnetron (top) and reduced cyclotron frequency (bottom) as a function of the quadrupolar excitation frequency (after a preceding dipolar magnetron excitation).

3.3. Octupolar excitation

While the measurements discussed above confirm well known and well understood excitation schemes, higher-order excitation schemes can be investigated, too, e.g., the octupolar excitation. The detailed structures of the resonance curves for the case of the octupolar excitation are presently under investigation. First experimental results by measurements with a ToF-effect technique have been reported recently [28,29]. In Fig. 7 an amplitude scan at the frequency $2\nu_c$ is shown, where the magnetron-signal intensity and cyclotron-signal intensity are plotted as a function of the excitation amplitude.

The signals show an oscillation. The general decrease of the signal intensities with increasing excitation amplitude is probably due to the damping of the ion motion by collisions with Ar atoms from the background gas.

In Fig. 8 the signal intensities at the magnetron and the cyclotron frequency are plotted as a function of the excitation frequency around the expected resonance at $2\nu_c$. For this study, an excitation amplitude was chosen, which corresponds to a full conversion with the octupolar excitation. The resonance frequency may be determined from the prominent peak at 3819.4 kHz. In analogy, the magnetron signal decreases to the noise level at the same frequency. Since a strong phase depen-

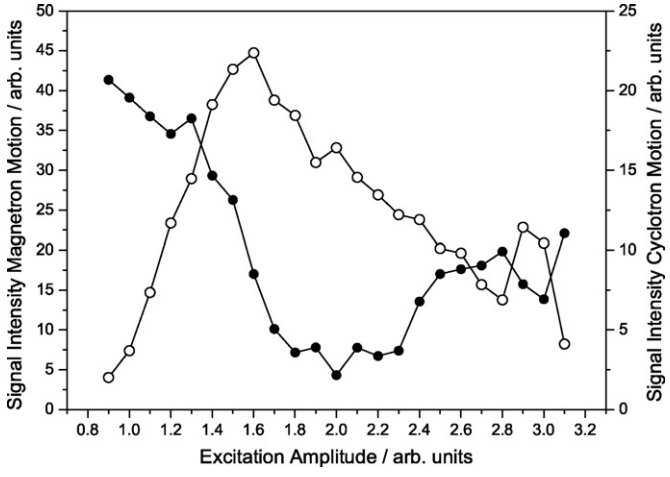

Fig. 7. Signal intensity at the magnetron (full circles) and reduced cyclotron frequency (open circles) as a function of the octupolar excitation amplitude.

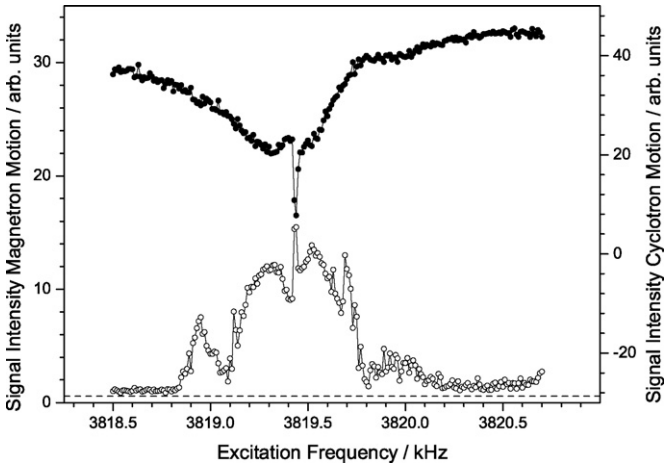

Fig. 8. Signal intensity at the magnetron (full circles) and the reduced cyclotron frequency (open circles) as a function of the octupolar excitation frequency (after a preceding dipolar rf excitation of the magnetron motion).

dence is expected [28,29,43,44], the phase between the dipolar excitation of the magnetron motion and the octupolar excitation for the conversion was kept constant. Taking the central peak for the determination of the resonance frequency, the FWHM is about 20 Hz, which is a factor 5 lower than the FWHM in case of a quadrupolar excitation with the same excitation duration of 10 ms. While the resonance curves show interesting features such as broader as well as small-scale structures and an indication of an asymmetry, a deeper investigation has only just begun [28,29,43,44] and it would be premature to speculate about particular details.

4. Conclusion and outlook

It has been shown that the standard dipolar FT-ICR detection technique can be applied to monitor the radial ion motions and their manipulation in a Penning trap. This broad-band detection scheme does not require the knowledge of the exact eigenfrequencies, i.e., frequency shifts may be monitored as well. In particular, the conversion from one radial mode to the other was probed by simultaneous monitoring the signal intensity of the magnetron and cyclotron motion. Both modes play important roles in high-precision mass spectrometry. The present method may not be directly applicable to short-lived nuclides and other exotic particles [45,46,47]. However, it can be combined with narrowband methods for increased sensitivity [48] and in any case it can be expected to be a useful tool in the elucidation of novel ion cyclotron resonance excitation schemes.

Acknowledgements

This work was supported by the Collaborated Research Centre SFB652 of the Deutsche Forschungsgemeinschaft, the German Ministry for Education and Research (BMBF) under contract 06GF186I, and the GSI research and development program. Furthermore, the authors thank the Max-Planck-Institute for Plasma Physics, IPP, Greifswald, for its kind hospitality.

References

[1] M.B. Comisarow, A.G. Marshall, Chem. Phys. Lett. 25 (1974) 282.
[2] I.J. Amster, J. Mass Spectrom. 31 (1996) 1325.
[3] A.G. Marshall, C.L. Hendrickson, G.S. Jackson, Mass Spectrom. Rev. 17 (1998) 1.
[4] A.G. Marshall, C.L. Hendrickson, Int. J. Mass Spectrom. 215 (2002) 59.
[5] B. Odem, D. Hanneke, B. D'Urso, G. Gabrielse, Phys. Rev. Lett. 97 (2006) 030801.
[6] T. Beier, H. Haffner, N. Hermanspahn, S.G. Karshenboim, H.-J. Kluge, W. Quint, S. Stahl, J. Verdu, G. Werth, Phys. Rev. Lett. 88 (2002) 011603.
[7] S. Rainville, J.K. Thompson, D.E. Pritchard, Science 303 (2004) 334.
[8] R.S. Van Dyck, S.L. Zafonte, S. Van Liew, D.B. Pinegar, P.B. Schwinberg, Phys. Rev. Lett. 92 (2004) 220802.
[9] G. Gabrielse, X. Fei, L.A. Orozco, R.L. Tjoelker, J. Haas, H. Kalinowsky, T.A. Trainor, W. Kells, Phys. Rev. Lett. 65 (1990) 1317.
[10] L.S. Brown, G. Gabrielse, Rev. Mod. Phys. 58 (1986) 233.
[11] L. Schweikhard, M. Blundschling, R. Jertz, H.-J. Kluge, Int. J. Mass Spectrom. Ion Process. 89 (1989) R7.
[12] L. Schweikhard, M. Blundschling, R. Jertz, H.-J. Kluge, Rev. Sci. Instrum. 60 (1989) 2631.
[13] L. Schweikhard, M. Lindinger, H.-J. Kluge, Rev. Sci. Instrum. 61 (1990) 1055.
[14] L. Schweikhard, M. Lindinger, H.-J. Kluge, Int. J. Mass Spectrom. Ion Process. 98 (1990) 25.
[15] L. Schweikhard, Rapid Commun. Mass Spectrom. 4 (1990) 360.
[16] Y. Pan, D.P. Ridge, A.L. Rockwood, Int. J. Mass Spectrom. Ion Process. 84 (1988) 293.
[17] E.N. Nikolaev, M.V. Gorshkov, A.V. Mordehai, V.L. Talrose, Rapid Commun. Mass Spectrom. 4 (1990) 144.
[18] P.A. Limbach, P.B. Grosshans, A.G. Marshall, Int. J. Mass Spectrom. Ion Process. 123 (1993) 41.
[19] M. Knobeler, K.P. Wanczek, Int. J. Mass Spectrom. Ion Process. 125 (1993) 127.
[20] M. Allemann, H.P. Kellerhals, K.-P. Wanczek, Chem. Phys. Lett. 84 (1981) 547.
[21] P.B. Grosshans, A.G. Marshall, Int. J. Mass Spectrom. Ion Process. 107 (1991) 49.
[22] P.A. Limbach, L. Schweikhard, K.A. Cowen, M.T. McDermott, A.G. Marshall, J.V. Coe, J. Am. Chem. Soc. 113 (1991) 6795.
[23] L. Schweikhard, A.G. Marshall, J. Am. Soc. Mass Spectrom. 4 (1993) 433.
[24] S. Guan, H.S. Kim, A.G. Marshall, M.C. Wahl, T.D. Wood, X. Xiang, Chem. Rev. 94 (1994) 2161.
[25] V.L. Campbell, Z. Guan, D.A. Laude, J. Am. Soc. Mass Spectrom. 7 (1995) 564.
[26] S. Guan, M.C. Wahl, T.D. Wood, A.G. Marshall, Anal. Chem. 65 (1993) 1753.
[27] G. Bollen, R.B. Moore, G. Savard, H. Stolzenberg, J. Appl. Phys. 68 (1990) 4355.
[28] R. Ringle, G. Bollen, P. Schury, S. Schwarz, T. Sun, Int. J. Mass Spectrom. 262 (2007) 33.
[29] S. Eliseev, M. Block, A. Chaudhuri, F. Herfurth, H.-J. Kluge, A. Martin, C. Rauth, G. Vorobjev, Int. J. Mass Spectrom. 262 (2007) 45.
[30] S. Becker, K. Dasgupta, G. Dietrich, H.-J. Kluge, S. Kuznetsov, M. Lindinger, K. Lützenkirchen, L. Schweikhard, J. Ziegler, Rev. Sci. Instrum. 66 (1995) 4902.
[31] L. Schweikhard, S. Krückeberg, K. Lützenkirchen, C. Walther, Eur. Phys. J. D 9 (1999) 15.
[32] L. Schweikhard, S. Becker, K. Dasgupta, G. Dietrich, H.-J. Kluge, D. Kreisle, S. Krückeberg, S. Kuznetsov, M. Lindinger, K. Lützenkirchen, B. Obst, C. Walther, H. Weidele, J. Ziegler, Phys. Scr. T59 (1995) 236.
[33] L. Schweikhard, A. Herlert, M. Vogel, in: E.E.B. Campbell, M. Larsson (Eds.), Proceedings of the Nobel Symposium on The Physics and Chemistry of Clusters, vol. 117, World Scientific, Singapore, 2001, p. 267.
[34] L. Schweikhard, A. Herlert, G. Marx, K. Hansen, in: J.-P. Connerade, A.V. Solov'yov (Eds.), Latest Advances in Atomic Clusters Collision: Atomic

Cluster Collisions: fission, fusion, electron, ion and photon impact, Imperial College Press, World Scientific, London, 2004, p. 85.
[35] S. Haebel, M.E. Walser, T. Gaumann, Int. J. Mass Spectrom. Ion Process. 151 (1995) 97.
[36] L.J. Dekoning, R.H. Fokkens, F.A. Pinkse, N.M.M. Nibbering, Int. J. Mass Spectrom. Ion Process. 77 (1987) 95.
[37] C.L. Hendrickson, J.J. Drader, D.A. Laude, J. Am. Soc. Mass Spectrom. 6 (1995) 448.
[38] L. Schweikhard, M. Breitenfeldt, A. Herlert, F. Martinez, G. Marx, N. Walsh, in: M. Drewsen, U.I. Uggerhoj, H. Knudsen (Eds.), Non-Neutral Plasma Physics VI: AIP Conf. Proc. 862, New York, 2006, p. 264.
[39] G.S. Jackson, C.L. Hendrickson, B.B. Reinhold, A.G. Marshall, Int. J. Mass Spectrom. 165 (1997) 327.
[40] R.D. Knight, Int. J. Mass Spectrom. Ion Process. 51 (1983) 127.
[41] A.G. Marshall, F.R. Verdun, Fourier Transforms in NMR, Optical and Mass Spectrometry, Elsevier, Amsterdam, 1990.
[42] R.S. Van Dyck, F.L. Moore, D.L. Farnham, P.B. Schwinberg, Phys. Rev. A 40 (1989) 6308.
[43] S. Schwarz, G. Bollen, D. Lawton, P. Lofy, D.J. Morrissey, J. Ottarson, R. Ringle, P. Schury, T. Sun, V. Varentsov, L. Weissman, Nucl. Instrum. Meth. B 204 (2003) 507.
[44] S. Baruah, Dissertation, in preparation.
[45] D. Lunney, J.M. Pearson, T. Thibault, Rev. Mod. Phys. 75 (2003) 1021.
[46] K. Blaum, Phys. Report 425 (2006) 1.
[47] L. Schweikhard, G. Bollen (Eds.), Ultra-accurate mass spectrometry and related topics, special issue of Int. J. Mass Spectrom. 251 (2/3) (2006).
[48] C. Weber, K. Blaum, M. Block, R. Ferrer, F. Herfurth, H.-J. Kluge, C. Kozhuharov, G. Marx, M. Mukherjee, W. Quint, S. Rahaman, S. Stahl, the SHITRAP Collaboration, Eur. J. Phys. A 25 (s01) (2005) 65.